# CORRECTED SQUEEZED-FILM DAMPING SIMULATION VALIDATED WITH A LORENTZ-FORCE MAGNETOMETER OPERATING IN VACUUM

*Alexandre Sinding[1], Ilker E. Ocak[2], Wajih U. Syed[3], Aveek N. Chatterjee[4], Christopher Welham[1], Shuangqin Liu[5], Jun Yan[5], Stephen Breit[5], Hyun-Kee Chang[2], Ibrahim (Abe) M. Elfadel[3], and Zouhair Sbiaa[4]*

[1]Coventor SARL, Villebon-sur-Yvette, FRANCE

[2]Institute of Microelectronics, A*STAR (Agency for Science, Technology and Research), SINGAPORE

[3]Masdar Institute of Science and Technology, Abu Dhabi, UAE

[4]GLOBALFOUNDRIES, SINGAPORE

[5]Coventor, Inc., Waltham, MA, USA

## ABSTRACT

A number of corrections to the well-known squeezed-film gas damping model are required to get accurate results for MEMS. This paper reports on the implementation and validation of a corrected squeezed-film damping (SFD) simulation for common MEMS structures, electrostatic comb fingers, under various vacuum levels. Experimental *Q* factors were measured for the first in-plane resonant mode of a Lorentz-force magnetometer. An acoustic boundary condition was implemented to accommodate, in different areas of the sensor, various ratios *a/h* of squeezing surface characteristic dimension *a* to squeezed gas gap *h*. At a typical operating pressure for this sensor, e.g. 10Pa, corresponding to Knudsen number *Kn* ~ 670, the simulated *Q* factor is within +/-25% of the measured value. This new, corrected simulation approach provides, for the first time, a practical and accurate way of predicting *Q* factors for complex capacitive MEMS sensors such as accelerometers, gyroscopes and magnetometers that operate at low pressure.

## INTRODUCTION

### Lorentz-force Magnetometer

Magnetometers are essential components for providing navigation and location-based services in mobile devices such as smart phones, tablets, and wearables. While magneto-resistive and Hall-effect magnetometers are the dominant technologies in existing electronic compasses, Lorentz-force magnetometers have notable advantages, including (1) no requirement of any specialized magnetic material, (2) no need of magnetic concentrators to sense fields parallel to the device, and (3) easy chip-scale integration with MEMS gyroscopes and accelerometers currently used in consumer electronics. We previously reported such a magnetometer integrated with a 6 degree-of-freedom monolithic inertial MEMS [1].

As shown in Figure 1, an AC excitation current at the mechanical resonant frequency is applied to the sensor, and the magnetic field strength is measured by monitoring the change in the amplitude of the sensor's resonant motion, by means of changes of electrostatic comb capacitance. It can be shown that sensitivity is proportional to the *Q* factor of the resonance, Brownian noise density is inversely proportional to the square root of *Q*, and sensing bandwidth is inversely proportional to *Q* [2]. In other words, *Q* factor is one of the most critical design parameters.

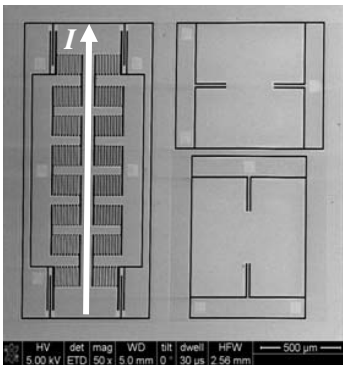


*Figure 1: SEM image of a 3-axis Lorentz-force magnetometer: Bz sensor (left); By sensor (right top); and Bx sensor (right bottom). Arrow indicates the drive current direction for the Bz sensor.*

### Compact Finite Element Analysis (FEA)

This work describes an enhancement to Coventor's *MEMS+*® software [3] which is used to design and simulate a variety of MEMS devices including the subject magnetometer, and to co-simulate MEMS devices with CMOS circuits and packaging effects.

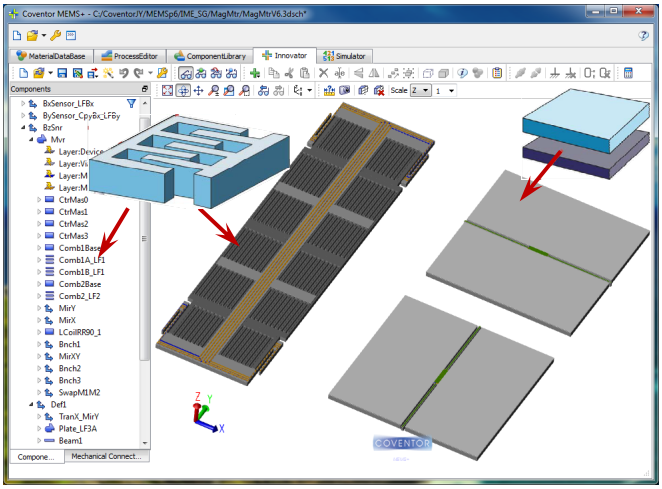

*Figure 2: Magnetometer model in MEMS+, assembled from parametric library components including rectangular plates and electrostatic combs.*

*MEMS+* includes a library of MEMS-specific, parametric finite elements. MEMS designers assemble these elements into a desired structure. Assembly can be done either in the *MEMS+* graphical user interface, as illustrated in Figure 2, or using MATLAB® scripting. The resulting models have relatively fewer elements compared to typical FEA, hence the description "compact FEA" is used. Other physics, including electrostatics and SFD effects are coupled to mechanical elements via specialized electrostatic and fluidic connectors as illustrated in Figure 3. In this paper, we focus on an enhancement of the SFD model in *MEMS+*. SFD between the moving and fixed comb fingers of the subject magnetometer is believed to be the primary damping mechanism for the in-plane resonant mode.

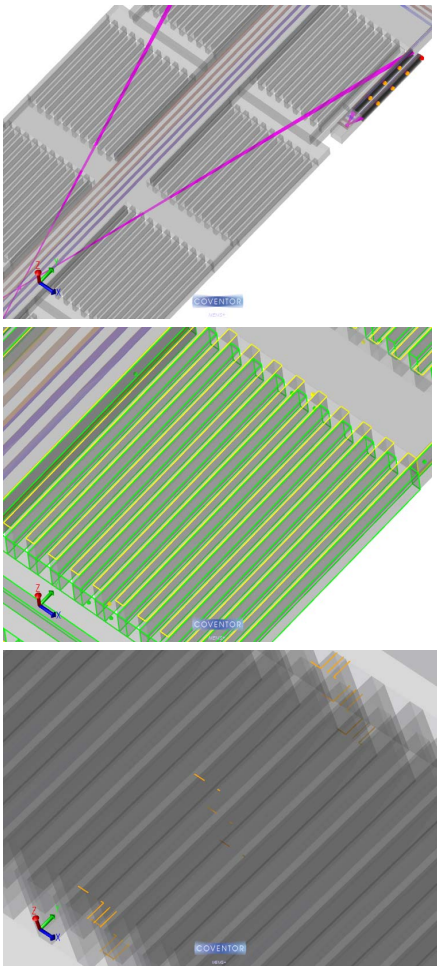

*Figure 3: MEMS+ multi-physics models have distinct connectors for the mechanical, electrical, and fluidic domains (from top to bottom).*

The ability to simulate *MEMS+* compact FEA models in the MATLAB, Simulink® and Cadence Virtuoso® environments has been reported previously [4], [5].

### Squeezed-Film Damping (SFD) Model

The SFD model replaces the 3D Navier-Stokes equation with the 2D Reynolds equation

$$\frac{P_0 h^3}{12\mu}\nabla^2\left(\frac{p}{P_0}\right) - h\frac{\partial}{\partial t}\left(\frac{p}{P_0}\right) = v \quad (1)$$

where $P_0$ is the ambient pressure, $h$ the thickness of the gap, $\mu$ the viscosity of the fluid, $p$ the pressure change in the gap, and $v$ the velocity of the movable plate. It has proven an efficient means of simulating gas damping [6]. However, corrections to the SFD model are required to get accurate results for MEMS, as described in the following sections.

## MODEL

### Correction with Acoustic Boundary Condition

The boundary conditions of Equation (1) are commonly set as $p=0$ for the edges of the gap. If so, SFD is only valid when the ratio of squeezing surface dimension $a$ to squeezed-gas gap $h$ is large, *i.e.* $a/h >> 10$. This assumption might or might not apply within a MEMS device. For example, the Lorentz-force magnetometer we are developing has $a/h \sim 7$ in some areas.

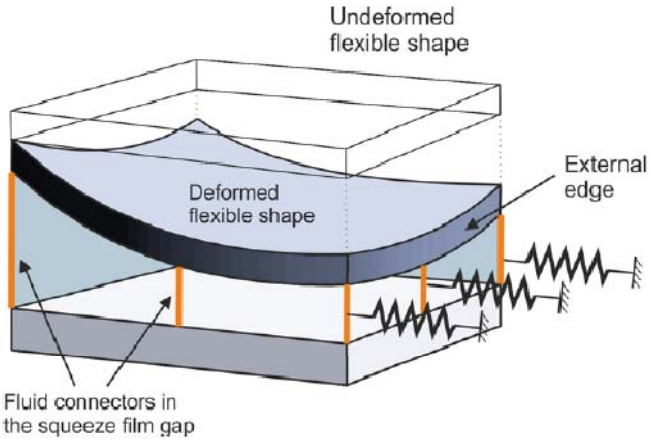


*Figure 4: Illustration of the acoustic boundary condition implementation in MEMS+: flow resistance added on an external edge.*

The SFD model in *MEMS+* has been corrected by applying an acoustic boundary condition that adds an additional flow resistance to all fluidic connectors on the edges of the comb fingers, as illustrated in Figure 4. Hence the boundary condition becomes:

$$\frac{\partial p}{\partial n} = \frac{p}{\Delta L} \quad (2)$$

where $\Delta L$ is the length of the edge on which the pressure drops linearly to zero, and $n$ is the outward normal. Furthermore, $\Delta L$ is adjusted as a function of $a/h$ [7].

### Correction for High Knudsen Number

SFD's gas continuum assumption is typically valid only when the Knudsen number $Kn$, the ratio of the mean free path of gas molecules to the gap $h$, is small, *i.e.* $Kn < 0.01$. Most resonance-based MEMS sensors such as gyroscopes operate in vacuum to achieve favorable $Q$ factors, and therefore have much larger $Kn$. For example, the Lorentz-force magnetometer under consideration operates at $Kn \sim 670$.

A correction to Equation (1) is to replace $\mu$ with an effective viscosity [8]:

$$\mu_{eff} = \frac{\mu}{1 + 9.638 K_n^{1.159}} \quad (3)$$

Furthermore, $\Delta L$ in Equation (2) can be corrected as a function of $Kn$ [9]. Both of these corrections have been implemented in the *MEMS*+ SFD model.

## MEASUREMENT AND SIMULATION

### Measurement of *Q* factor in Various Vacuum Levels

The $Q$ factors of the magnetometer's sensing modes were measured with a dynamic signal analyzer. This work focuses on the gas damping of the *Bz* sensing mode, which is an in-plane oscillation in the $x$ direction as shown in Figure 5. The *Bz* sensor's 3dB bandwidth was determined by taking its resonant peak point as the reference and then searching the -3dB points on the right and left side of the resonant peak. The $Q$ factor is the resonant frequency divided by the 3dB bandwidth. $Q$ factors over a range of vacuum levels were measured.

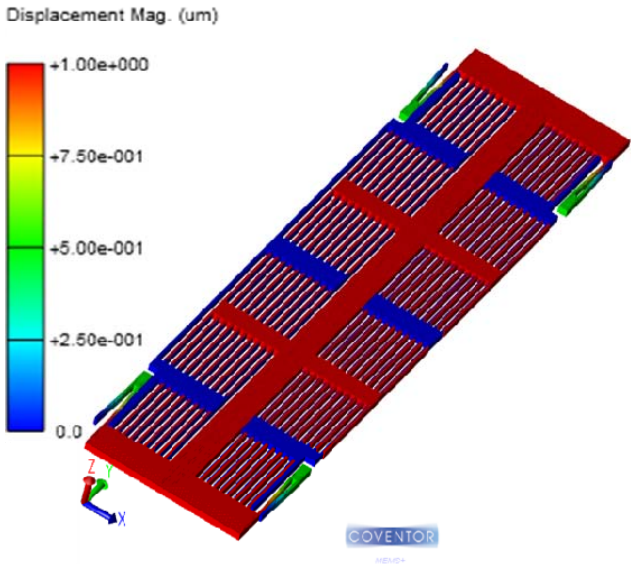


*Figure 5: FEA modal analysis result for the Bz sensor, which is driven by current in the y-direction (not shown in this figure). The simulated sensing mode is an in-plane +/- x translation at 12 kHz.*

### Model Setup

After implementing the SFD corrections mentioned in preceding sections, the *MEMS*+ analysis settings became straightforward as the "Edge Flow Condition: Automatic Elongation" option, as illustrated in Figure 6. Also as mentioned previously, all *MEMS*+ models are parametric, making it easy to analyze the $Q$ factor for various vacuum levels by changing the ambient pressure variable in the model.

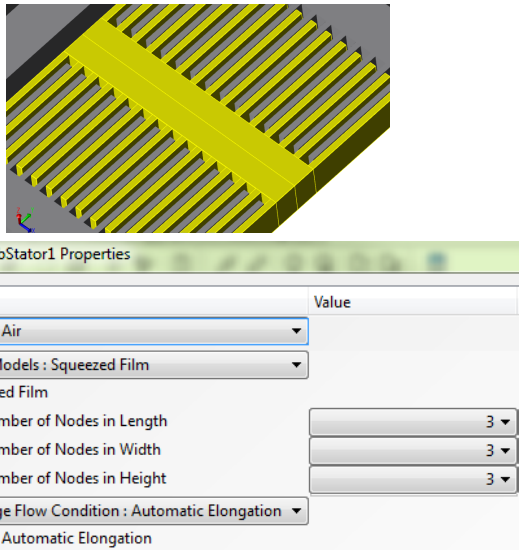


*Figure 6: Details of sensing comb (top) and the SFD simulation settings (bottom).*

## RESULTS AND DISCUSSION

### Validation of *Q*-factor Simulation

The simulated $Q$ factor is compared to the measured data in Figure 7. The $Q$ values calculated with the corrected SFD simulations are within +/-25% of the measured data over the pressure range of 1,000 Pa down to the typical sensor operating pressure of 10 Pa, which corresponds to $Kn$ ~ 670 for the *Bz* sensor.

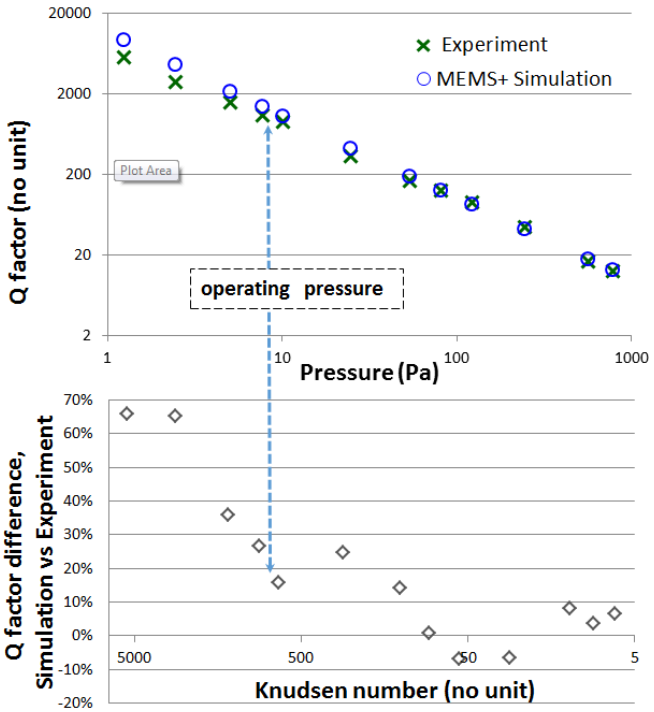


*Figure 7: Bz sensor Q factor simulation versus experiment. Sensor operating pressure is around 10Pa.*

With this validation, we expect that the corrected SFD model provides, for the first time, an efficient and accurate

way of predicting *Q* factors for complex capacitive MEMS sensors such as gyroscopes and magnetometers that operate in typical vacuum conditions. Even at higher *Kn*, up to 5,000, the corrected SFD predicts *Q* factors within an order-of-magnitude (simulated vs. measured values are within 70%), which is still useful for designing similar types of sensors.

**Practical and Accurate Way of Predicting *Q* factor**

Accurately predicting *Q* factor with conventional FEA is computationally challenging because the fluidic domain must be discretized with a fine mesh. Fortunately, if SFD is the main factor of the device damping, which is typically the case for capacitive MEMS sensors that employ large numbers of comb fingers to sense in-plane modes, the corrected SFD simulation reported herein is a practical and accurate way of predicting *Q* factor. As an example, simulating the 12 different pressure levels in Figure 7 took only about 5 minutes of wall-clock time on a laptop computer with an Intel® Core i7-series CPU and 16 GB of memory. For a complex device as shown in Figure 1, design optimization might require simulating thousands of different geometric configurations. Thanks to the compact modeling approach implemented in *MEMS*+, this level of *Q* factor optimization is now quite feasible.

It is emphasized that similar electrostatic comb fingers are widely used in other MEMS sensors such as accelerometers and gyroscopes, and therefore the corrected SFD model implemented in *MEMS*+ is expected to be helpful for designing those sensors as well.

## CONCLUSIONS

We report herein the implementation and validation of a corrected SFD model suitable for predicting *Q* factors for common MEMS structures under various vacuum levels. Experimental *Q* factor values were measured for the first in-plane resonant mode of a Lorentz-force magnetometer at different pressure levels. The predicted *Q* values agree well with the experimental values over a wide range of pressure values. At a typical operating pressure for the sensor under development, 10Pa, corresponding to Knudsen number *Kn* ~ 670, the simulated Q factor is within +/-25% of the measured value which may be considered sufficient accuracy for design purposes. Even at higher *Kn* values, up to 5,000, the corrected SFD model predicts *Q* factors within an order-of-magnitude (simulated vs. measured values are within 70%), which is still useful for designing these types of sensors.

This new, corrected simulation approach provides, for the first time, a practical and accurate way of predicting Q factors for complex MEMS sensors such as gyroscopes and magnetometers.

## ACKNOWLEDGEMENTS

This work was partially funded by Mubadala Development Company - Abu Dhabi, the Economic Development Board - Singapore, and GLOBALFOUNDRIES - Singapore under the framework of 'Twinlab' project with participation of A*STAR Institute of Microelectronics - Singapore, Masdar Institute of Science and Technology - Abu Dhabi and GLOBALFOUNDRIES - Singapore.

## REFERENCES

[1] I. Ocak, D. Cheam, S. Fernando, A. Lin, P. Singh, J. Sharma, G. Chua, B. Chen, A. Gu, N. Singh, D. Kwong, “A monolithic 9 degree of freedom (DOF) capacitive inertial MEMS platform”, in *IEEE International Electron Devices Meeting 2014*, pp. 22.6.1-22.6.4.

[2] V. Rouf, M. Li, D. Horsley, “Area-Efficient Three Axis MEMS Lorentz Force Magnetometer”, *IEEE Sensors J*, vol. 13, pp. 4474- 4481, 2013.

[3] G. Lorenz and G. Schröpfer, “3D Parametric-Library-Based MEMS/IC Design,” in *System-level Modeling of MEMS*, WILEY-VCH Verlag GmbH & Co. KGaA, 2013, pp. 407-424. Coventor.com also has up-to-date information of MEMS+.

[4] A. Parent, A. Krust, G. Lorenz, I. Favorskiy, T. Piirainen, “Efficient nonlinear simulink models of MEMS gyroscopes generated with a novel model order reduction method”, in *Transducers 2015, 18th International Conference*, pp. 2184-2187.

[5] A. Parent, A. Krust, G. Lorenz, T. Piirainen, “A novel model order reduction approach for generating efficient nonlinear Verilog-a models of MEMS gyroscopes", in *IEEE Inertial Sensors and Systems 2015, International Symposium*, pp. 1-4.

[6] M. Bao, H. Yang, “Squeeze film air damping in MEMS”, *Sensors and Actuators A: Physical*, vol. 136, pp. 3-27, 2007.

[7] T. Veijola, A. Pursula, P. Raback, “Extending the validity of squeezed-film damper models with elongations of surface dimensions”, *J Micromech Microeng*, vol 15, pp. 1624-1636, 2005.

[8] T. Veijola, H. Kuisma, J. Lahdenpera, “The Influence of Gas-Surface Interaction on Gas Film Damping in a Silicon Accelerometer”, *Sensors and Actuators A: Physical* , vol.66, pp.83-92, 1998.

[9] T. Veijola, “End Effects of Rare Gas Flow in Short Channels and in Squeezed-Film Dampers”, in *2002 International Conference on Modeling and Simulation of Microsystems*. pp. 104-107,

## CONTACT

* J. Yan, tel: +1-617-9458678; jyan@coventor.com